

Climate change hotspots in the United States

Noah S. Diffenbaugh^{1*}, Filippo Giorgi² and Jeremy S. Pal³

¹*Purdue Climate Change Research Center and Department of Earth and Atmospheric Sciences, Purdue University, 550 Stadium Mall Drive, West Lafayette, IN, 47907-2051, U.S.A.*

²*Abdus Salam International Centre for Theoretical Physics, Strada Costiera 11, I-34014 Trieste, Italy.*

³*Frank R. Seaver College of Science and Engineering, Loyola Marymount University, 1 LMU Drive MS 8135, Los Angeles, CA, 90045, U.S.A.*

*corresponding author

Noah S. Diffenbaugh

Department of Earth and Atmospheric Sciences

Purdue University

550 Stadium Mall Drive

West Lafayette, IN, 47906-2051

diffenbaugh@purdue.edu

(765) 464-8725 (telephone)

(765) 496-1210 (fax)

Abstract

We use a multi-model, multi-scenario climate model ensemble to identify climate change hotspots in the continental United States. Our ensemble consists of the CMIP3 atmosphere-ocean general circulation models, along with a high-resolution nested climate modeling system. We test both high (A2) and low (B1) greenhouse gas emissions trajectories, as well as two different statistical metrics for identifying regional climate change hotspots. We find that the pattern of peak responsiveness in the CMIP3 ensemble is persistent across variations in GHG concentration, GHG trajectory, and identification method. The high-resolution climate modeling system produces highly localized hotspots within the basic GCM structure, but with a higher sensitivity to the identification method. Across the ensemble, the pattern of relative climate change hotspots is shaped primarily by changes in interannual variability of the contributing variables rather than by changes in the long-term means.

1. Introduction

Observed late 20th century global warming has been attributed primarily to anthropogenic changes in radiative forcing of the climate system (e.g., [IPCC, 2007]), with further warming of approximately 1 to 6 °C likely to occur by the end of the 21st century [IPCC, 2007]. Precisely how this long-term global warming will manifest at smaller spatial and temporal scales is a key question for understanding, avoiding, and/or preparing for climate change. In particular, design and implementation of climate change mitigation and adaptation strategies requires quantification of potential spatial heterogeneity in the aggregate climate response. Therefore, there exists a need to identify climate change hotspots that are likely to be most responsive to anthropogenic changes in climate forcing, and to understand the mechanisms underlying the enhanced responsiveness in the hotspot regions.

Our analysis is focused on the continental United States (U.S.). The relative sensitivity of climate to greenhouse gas (GHG) forcing within the U.S. is important for a number of reasons. First, the U.S. encompasses a large continental area with a diversity of climatic regimes. In addition, it is home to a substantial human population and a large and diverse economy that is at least partly dependent on climate, including a large fraction of the global agricultural production. Further, the U.S. has become a significant party in climate change negotiations, both because it is one of the largest GHG emitters and because local and state governments are entering into climate agreements independent of Federal action (e.g., [Rabe, 2004]). The latter is particularly relevant for the identification of climate change hotspots within the United States, as the emergence

of the state government as a primary unit of climate policy action enhances the need for regional- and state-level climate change information [Rabe, 2004].

Climate change hotspots can be identified based on the magnitude of physical climate response (as in [Giorgi, 2006]) or on the vulnerability to climate change impacts (e.g., [Diffenbaugh, et al., 2007a]). Specific impact assessments can provide detailed quantification of the potential vulnerability of particular natural and human systems (e.g., [White, et al., 2006]). Although a framework does not yet exist for quantitatively exploring a large suite of possible impacts while also capturing the likely spatial complexity of physical climate change, measures of the net change within multivariate climate space can serve as a metric of the total responsiveness of different geographic areas, which can in turn provide a general indication of which areas might be faced with the greatest aggregate changes in physical climate stress in the coming decades. To date, such response-based hotspot identification has focused on global climate model assessment, using either statistical [Williams, et al., 2007] or subjective [Diffenbaugh, et al., 2007a; Giorgi, 2006] aggregation of multiple climate variables.

Here we focus on the physical response, employing statistical measures of aggregate climate change to identify regional climate change hotspots within the continental U.S. We explore the climate change uncertainty space by analyzing: (1) the CMIP3 multi-model atmosphere-ocean general circulation model (AOGCM) ensemble [IPCC, 2007], which allows us to examine the effect of different physical treatments of the climate system as well as different GHG emission scenarios; (2) two aggregated statistical metrics of climate change, which allows us to examine the sensitivity to the hotspot identification method; and (3) a high-resolution nested climate simulation, which

allows us to explore the importance of fine-scale processes in modulating the climate change signal. The last of these is important because both the magnitude (e.g., [Diffenbaugh, et al., 2007b; Diffenbaugh, et al., 2005]) and impacts (e.g., [White, et al., 2006]) of simulated climate change can vary substantially at sub-GCM grid-scales.

2. Models and Methods

2.1. Climate Model Data

We analyze AOGCM simulations from the CMIP3 multi-model archive. The CMIP3 models successfully capture the structure of temperature and precipitation over the continental United States [Randall, et al., 2007]. In order to test the sensitivity of our hotspot identification to GHG concentration, we analyze CMIP3 data from the A2 and B1 emission scenarios [IPCC, 2000]. The A2 and B1 socioeconomic pathways result in GHG concentrations at the higher and lower ends of the IPCC illustrative scenario range, respectively [IPCC, 2007]. In order to facilitate direct comparisons between the A2 and B1 ensemble simulations, we use results from 15 models archiving data for both scenarios.

In order to test the sensitivity of the hotspot identification to fine-scale climate processes, we employ the Abdus Salam International Center for Theoretical Physics Regional Climate Model (RegCM3) [Pal, et al., 2007]. RegCM3 is able to capture the climatology of temperature and precipitation over a number regions of the world (e.g., [Pal, et al., 2007]), including the United States (e.g., [Diffenbaugh, et al., 2006]). We use the simulations described in [Diffenbaugh, et al., 2005], [White, et al., 2006], and [Trapp, et al., 2007]. The model domain covers the conterminous United States and adjacent

ocean waters with a 25 km horizontal grid interval and 18 levels in the vertical. The RegCM3 simulations use atmospheric boundary conditions from the NASA finite volume GCM (FVGCM) simulations of [Coppola and Giorgi, 2005]. In this configuration, the global FVGCM grid has 1° horizontal resolution in latitude and 1.25° in longitude, with 18 levels in the vertical. In the reference simulation the models use observed monthly-varying SSTs, while in the future climate simulation a monthly-varying SST anomaly is added based on A2 scenario simulations with the HadCM3 AOGCM, as described in [Giorgi, et al., 2004]. Although the atmospheric boundary conditions provided by the FVGCM are equilibrated with the prescribed SSTs, inconsistencies between the atmospheric and SST fields could be introduced by the lack of two-way coupling between the atmosphere and ocean in the FVGCM simulations.

Finally, in order to examine the role of the large-scale boundary conditions in shaping the response of the high-resolution climate model, we also analyze the FVGCM simulations, using the reference period of 1961-1989 and the future period of 2071-2099 in the A2 scenario.

2.3. Hotspot Identification

The goal of this study is to develop metrics for comparing the relative responsiveness of different regions of the U.S. within a multivariate climate space. This hotspot identification requires aggregation of positive and negative changes in a number of climate variables of different scales and units. In order to meet this challenge, we use two statistical measures to identify climate change hotspots in the continental U.S. Our identification framework is based on that of [Giorgi, 2006], [Diffenbaugh, et al., 2007a]

and [Williams, et al., 2007]. Following [Giorgi, 2006], we quantify the aggregate response of mean and variability of seasonal temperature and precipitation. We calculate mean temperature and precipitation as the long-term average of each year’s seasonal mean. Following [Giorgi, 2006], we calculate temperature variability as the interannual standard deviation of the seasonal means, and precipitation variability as the interannual coefficient of variation of the seasonal means (the interannual standard deviation divided by the long-term mean), after first detrending the seasonal timeseries.

Following [Giorgi, 2006], [Diffenbaugh, et al., 2007a] and [Williams, et al., 2007], we separate each year into two seasons in order to capture sub-annual changes that could potentially cancel at the annual-scale (for instance, drying in one season and wetting in another). We follow [Giorgi, 2006] and [Diffenbaugh, et al., 2007a] in designating April through September and October through March as the two 6-month seasons for the continental U.S. These also encompass the June-July-August and December-January-February seasons of [Williams, et al., 2007]. We aggregate the different seasons by treating them as different variables, yielding eight total variables to be used in our aggregation metrics (long-term mean and variability of warm- and cold-season temperature and precipitation).

We employ two hotspot identification metrics. The first follows [Williams, et al., 2007] in employing the Standard Euclidean Distance (SED) to measure the distance traveled in multivariate climate space. At each land grid point, we calculate the total SED between the future (f) and present (p) periods as:

$$SED_{fp} = \text{sqrt}(\sum_v SED_v) \quad (1)$$

for

$$SED_v = (x_{fv} - x_{pv})^2 / (\text{mean}[\text{abs}(x_{fv} - x_{pv})]_{ij})^2 \quad (2)$$

where x_{fv} is the value of variable v in the future period, x_{pv} is the value of variable v in the reference period, and $\text{mean}[\text{abs}(x_{fv} - x_{pv})]_{ij}$ is the mean of the absolute value of land-grid-point change for variable v over all land grid points ij . The denominator in Eq. (2) is used to normalize the metric. We find that using a regional or global domain in the denominator yields similar results (not shown).

As an additional metric, we use the squared cord distance dissimilarity coefficient (SCD) of [Overpeck, et al., 1992]. The SCD quantifies the dissimilarity between sample populations. At each land grid point, we calculate the total SCD between the future (f) and present (p) periods as the sum of the SCD scores for each variable v :

$$SCD_{fp} = (\sum_v SCD_v) \quad (3)$$

for

$$SCD_v = ([x_{fv}^{1/2} - x_{pv}^{1/2}]^2) / \text{S.D.}([x_{fv}^{1/2} - x_{pv}^{1/2}]_{ij}) \quad (4)$$

where $\text{S.D.}([x_{fv}^{1/2} - x_{pv}^{1/2}]_{ij})$ is the standard deviation of the land-grid-point dissimilarity values for variable v over all land grid points ij . Because we normalize the SED values by the grid-point mean, we instead normalize the SCD values by the grid-point standard deviation in order to explore the sensitivity of the hotspot identification to the details of the identification method.

In aggregating the different models in the CMIP3 ensemble, we first calculate the eight variables for each model individually, then calculate the mean value of each variable from all of the models, and then calculate the aggregate metrics using those multi-model mean values of the eight variables.

3. Results

The CMIP3 ensemble dataset shows peak SED scores (i.e., hotspots) over southern California, northern Mexico, and western Texas (Figure 1). Minimum CMIP3 SED scores occur over the Gulf Coast and Atlantic Coast regions, as well as the northern Great Plains. The FVGCM dataset shows SED peaks over central California, northern Mexico, and western Texas, although these are more localized than in the CMIP3 dataset. In addition, the FVGCM shows relatively high SED scores over the Midwestern U.S. and minimum SED scores over the southeastern and northwestern U.S. The RegCM3 dataset shows highly localized peak SED scores over southern California, western Arizona, northern Mexico and the Atlantic Coast, along with secondary peaks over the Midwestern U.S. The SCD scores show generally similar patterns as the SED scores for all three datasets. Key exceptions include muting of the central California hotspot in the FVGCM simulations, and enhancement of the Midwestern hotspot in all three datasets.

The pattern of SED hotspots is shaped more by changes in interannual variability than by changes in the long-term mean of the contributing variables (Figure 2). For instance, the two most prominent contributors to the CMIP3 southern California hotspot are the two seasonal precipitation variability variables, and the three most prominent contributors to the CMIP3 northern Mexico and western Texas hotspots are the two seasonal precipitation variability variables and October-March temperature variability (along with April-September mean precipitation over northern Texas). Likewise, the primary contributors to the FVGCM central California and western Texas hotspots are the two seasonal precipitation variability variables, and the two most prominent contributors to the FVGCM SED Midwestern hotspot are the two seasonal temperature

variability variables. Additionally, the primary contributors to the RegCM3 southern California and western Arizona SED hotspots are the two precipitation variability variables. Across the simulations, warm-season variability is generally a stronger contributor than cold-season variability (Figure 2).

The pattern of SED hotspots shows little sensitivity to either the time evolution or the total concentration of atmospheric GHGs (Figure 3). For instance, in both the A2 and B1 emissions scenarios, southern California, western Texas, and northern Mexico emerge with the highest SED scores in the late 21st century, with the southeastern U.S. and northern Great Plains showing the lowest SED scores. Likewise, this is the basic hotspot pattern in both scenarios throughout the 21st century. Notable exceptions include a narrowing of the southern California hotspot in the early 21st century of the A2 CMIP3 dataset, as well as a slight westward migration of the Texas hotspot in the late 21st century of the A2 CMIP3 dataset.

4. Discussion and Conclusions

The pattern of climate change hotspots in the United States is generally persistent in the CMIP3 multi-AOGCM ensemble. Southern California, northern Mexico, and western Texas show the greatest climate change responsiveness in the late-21st century using either of the identification methods that we have applied. The Midwest region also shows relatively high hotspot metric values, while the Gulf Coast and Atlantic Coast regions show the least responsiveness (Figure 1). Similarly, the pattern of responsiveness is largely consistent between high- and low-end emissions scenarios, and throughout the 21st century (Figure 3). This pattern is mostly in place even in the early 21st century,

when differences in GHG forcing are relatively small compared to present and the inter-model variability could damp the climate change signal. This persistence of the hotspot pattern in the CMIP3 ensemble suggests that the broad patterns of climate responsiveness may be robust to climate system variability. (Whether the patterns are robust to model formulation requires further analysis.)

It is also notable that a single FVGCM realization not included in the CMIP3 ensemble displays a number of features seen in that ensemble (particularly for the SED metric; Figure 1). FVGCM does show considerably more sensitivity to the hotspot identification method (as does RegCM3), particularly over California and the Midwestern United States. This sensitivity of the single realization to the identification method could indicate that multiple realizations using multiple climate models are required in order to generate reliable projections of relative regional climate sensitivity. In addition, the fact that the FVGCM dataset consists of only one realization could explain the strength of the Midwestern hotspot in the FVGCM dataset relative to the CMIP3 dataset, with multiple realizations in the CMIP3 ensemble potentially damping the magnitude of changes in seasonal temperature variability (Figure 2). Alternatively, the relatively fine horizontal resolution of the FVGCM grid could also contribute to deviations from the CMIP3 ensemble. Likewise, whereas the CMIP3 ensemble consists of coupled atmosphere-ocean GCM simulations, the FVGCM realization was generated using prescribed SSTs synthesized by adding simulated SST changes to an observational SST timeseries (as described in [Giorgi, *et al.*, 2004]).

The pattern of SED and SCD scores in the RegCM3 simulations highlights the limitations of applying high-resolution climate models to statistical climate change

hotspot identification. Although the RegCM3 simulations reveal high scores within some of the areas identified in the GCM simulations, those hotspot areas are highly localized, with considerably lower scores elsewhere in the domain (Figure 1). This localization is also seen in the contributing variables, with a large range between the few grid-points showing maximum values and the vast majority of grid-points showing minimum values (Figure 2). Some of the differences between the RegCM3 and CMIP3 patterns can be linked to the forcing by the FVGCM (such as the relatively high SCD and SED values over the Midwestern U.S.). However, the overall pattern in the RegCM3 simulations deviates more from the driving FVGCM than the FVGCM deviates from the CMIP3 ensemble, highlighting the need for multiple realizations with multiple GCM-RCM combinations in order to generate robust high-resolution hotspot identification.

Peak aggregate climate changes in all three climate model datasets are driven primarily by changes in interannual variability, particularly of precipitation. This dominance of variability results from the fact that there is more inter-grid-point heterogeneity in the changes in variability than in the changes in seasonal mean. The fact that the hotspot distribution is strongly influenced by changes in precipitation variability highlights the importance of accurate modeling of cloud and precipitation processes. Further, non-hotspot areas should not be considered to be immune from climate change, as the climatic changes projected here could have substantial impact in areas that are not identified as response hotspots (e.g., [Trapp, *et al.*, 2007; White, *et al.*, 2006]).

5. Acknowledgements

We thank two anonymous reviewers for insightful and constructive comments. The RegCM3 simulations were generated using computational resources in the Rosen Center for Advanced Computing at Purdue University. This work was supported in part by NSF awards 0450221 and 0315677.

6. References

- Coppola, E., and F. Giorgi (2005), Climate change in tropical regions from high-resolution time-slice AGCM experiments, *Quarterly Journal of the Royal Meteorological Society*, *131*, 3123-3145.
- Diffenbaugh, N. S., et al. (2006), Summer aridity in the United States: Response to mid-Holocene changes in insolation and sea surface temperature, *Geophys. Res. Lett.*, *33*, L22712, doi:22710.21029/22006GL028012.
- Diffenbaugh, N. S., et al. (2007a), Indicators of 21st century socioclimatic exposure, *Proceedings of the National Academy of Sciences of the United States of America*, *104*, 20195-20198.
- Diffenbaugh, N. S., et al. (2007b), Heat stress intensification in the Mediterranean climate change hotspot, *Geophys. Res. Lett.*, *34*, L11706, doi:11710.11029/12007GL030000.
- Diffenbaugh, N. S., et al. (2005), Fine-scale processes regulate the response of extreme events to global climate change, *Proceedings of the National Academy of Sciences of the United States of America*, *102*, 15774-15778.
- Giorgi, F. (2006), Climate change hot-spots, *Geophys. Res. Lett.*, *33*, L08707, doi:08710.01029/02006GL025734.
- Giorgi, F., et al. (2004), Mean, interannual variability and trends in a regional climate change experiment over Europe. II: climate change scenarios (2071-2100), *Clim. Dyn.*, *23*, 839-858.
- IPCC, W. G. I. (2000), *Special Report on Emissions Scenarios*, 570 pp., Cambridge University Press, Cambridge, UK.

- IPCC, W. G. I. (2007), *Climate Change 2007: The Physical Science Basis: Contribution of Working Group I to the Fourth Assessment Report of the Intergovernmental Panel on Climate Change*.
- Overpeck, J. T., et al. (1992), Mapping eastern North American vegetation change of the past 18 ka: no-analogs and the future, *Geology*, *V20*, 1071-1074.
- Pal, J. S., et al. (2007), Regional climate modeling for the developing world: the ICTP RegCM3 and RegCNET, *Bull. Amer. Meteorol. Soc.*, *89*, 1395-1409.
- Rabe, B. (2004), *Statehouse and Greenhouse*, Brookings Institution Press, Washington, D.C.
- Randall, D. A., et al. (2007), Climate Models and Their Evaluation, in *Climate Change 2007: The Physical Science Basis. Contribution of Working Group I to the Fourth Assessment Report of the Intergovernmental Panel on Climate Change*, edited by S. Solomon, et al., Cambridge, United Kingdom and New York, NY, USA.
- Trapp, R. J., et al. (2007), Changes in severe thunderstorm environment frequency during the 21st century caused by anthropogenically enhanced global radiative forcing, *Proceedings of the National Academy of Sciences*, *104*, 19719-19723.
- White, M. A., et al. (2006), Extreme heat reduces and shifts United States premium wine production in the 21st century, *Proceedings of the National Academy of Sciences*, *103*, 11217-11222.
- Williams, J. W., et al. (2007), Projected distributions of novel and disappearing climates by 2100AD, *Proceedings of the National Academy of Sciences*, *104*, 5738-5742.

7. Figure Captions

Figure 1. Aggregate climate change scores in the United States. Top row shows aggregate scores using the Standard Euclidean Distance (SED). Bottom row shows aggregate scores using the Squared Cord Distance (SCD). Unitless.

Figure 2. Variables contributing to aggregate climate change hotspots in the United States. The four variables making the highest contribution to the Standard Euclidean Distance (SED) hotspots identified in Figure 1 are shown for each of the climate model datasets. In order to most readily compare the variable contributions with the net SED value, we show the square root of the individual SED_v variable scores (see Equation 2). Top row shows variables contributing to the CMIP3 hotspots. Middle row shows variables contributing to the FVGCM hotspots. Bottom row shows variables contributing to the RegCM3 hotspots. Unitless.

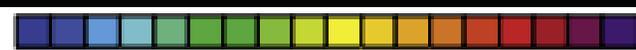
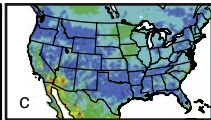
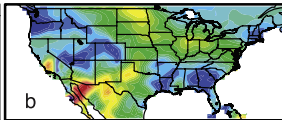
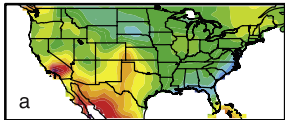
Figure 3. Sensitivity of aggregate climate change scores to greenhouse gas concentration and pathway. The aggregate Standard Euclidean Distance (SED) scores are shown for three three-decade periods of the 21st century. Top row shows results for the A2 emissions scenario. Bottom row shows results for the B1 emissions scenario. Unitless.

CMIP3

FVGCM

RegCM3

SED



2 3 4 5

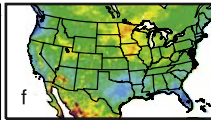
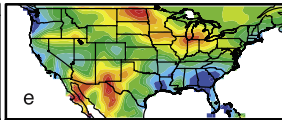
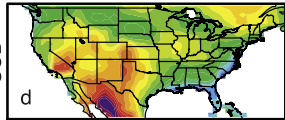


2 3 4 5 6 7



2 4 6 8 10 12

SCD



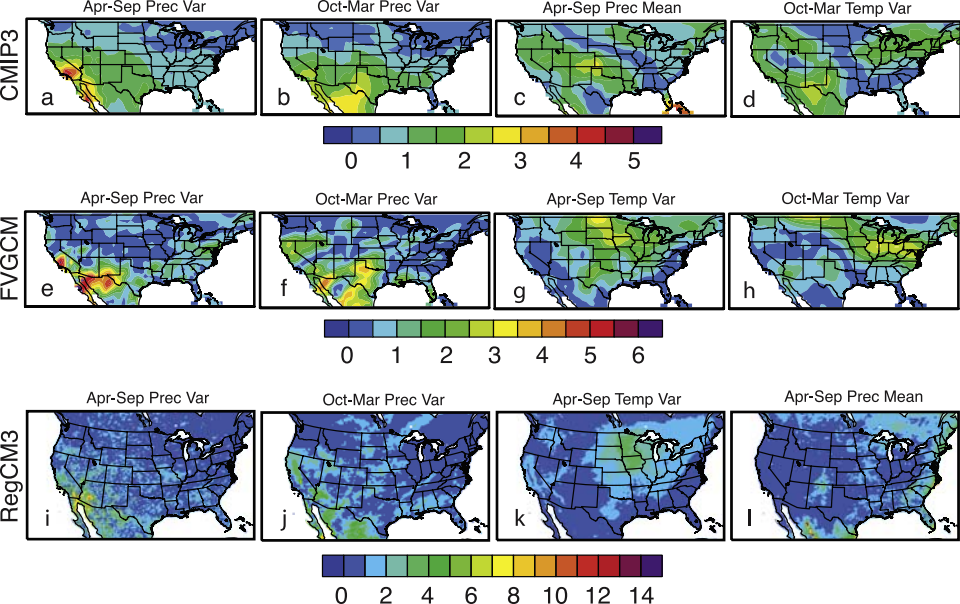
6 10 14 18 22



4 8 12 16



4 8 12 16 20

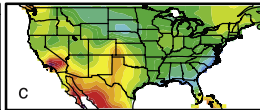
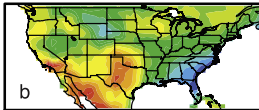
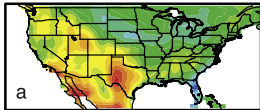


2011-2040

2041-2070

2071-2099

A2

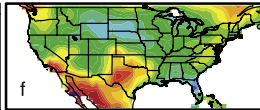
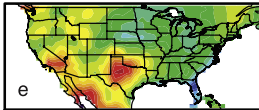
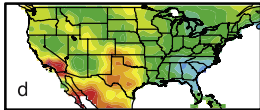


a

b

c

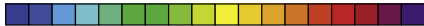
B1



d

e

f



2.0

3.0

4.0

5.0